
Article:
Dickinson, A., Bruyns-Haylett, M., Jones, M. et al. (1 more author) (2015) Increased peak gamma frequency in individuals with higher levels of autistic traits. European Journal of Neuroscience, 41 (8). pp. 1095-1101. ISSN 0953-816X

https://doi.org/10.1111/ejn.12881

Journal Section: Cognitive Neuroscience

Increased peak gamma frequency in individuals with higher levels of autistic traits

Abigail Dickinson[1], Dr Michael Bruyns-Haylett[2], Dr. Myles Jones[1] and Dr. Elizabeth Milne[1]

[1.] Department of Psychology, University of Sheffield, Western Bank, Sheffield, S10 2TP, UK.

[2.]School of Systems Engineering, University of Reading, Whiteknights, Reading, RG6 6AY, UK.

Corresponding author: Abigail Dickinson, Department of Psychology, University of Sheffield, Western Bank, Sheffield, S10 2TP, UK. Tel: 07854111433. Email: a.dickinson@sheffield.ac.uk.

Running Title: Peak gamma frequency and autistic traits.

Number of pages: 21.

Number of figures: 3.

Number of tables: 0.

Number of equations: 2.

Article body length: 3929 words.

Abstract Length: 220 words.

Introduction Length: 448 words.

Key Words: autism; electroencephalography; gamma activity; perception; individual differences.

Abstract

Individual differences in orientation discrimination threshold are related to both visually-induced peak gamma frequency and the presence of autistic traits. The relationship between peak gamma frequency and orientation discrimination thresholds may be due to both of these factors being mediated by levels of neural inhibition. No study has previously measured the relationship between peak gamma frequency and levels of autistic traits. Thus, this was the aim of the present study.

We measured orientation discrimination thresholds and autistic traits in a neurotypical human sample (N=33), and separately recorded electroencephalography to measure visually induced gamma activity. In line with our prediction, we found a significant relationship between peak gamma frequency and level of autistic traits. Consistent with previous work we also found significant relationships between orientation discrimination thresholds and level of autistic traits and between orientation discrimination thresholds and peak gamma frequency.

Our results demonstrate that individuals with individuals with higher levels of autistic personality traits have a higher peak-gamma frequency and are better at discriminating between visual stimuli based on orientation. As both higher peak gamma frequency and lower orientation discrimination thresholds have been linked to higher levels of neural inhibition, this suggests that autistic traits co-occur with increased neural inhibition. This discovery is significant as it challenges the currently-held view that autism spectrum conditions are associated with increased neural excitation.

Introduction

Visual perception varies considerably between individuals. Individual differences are evidenced by variability in sensory discrimination thresholds measured by a range of psychophysical tasks including contrast sensitivity, wavelength discrimination, Vernier acuity and orientation discrimination (Edden et al., 2009; Halpern et al., 1999). In relation to orientation discrimination, we have previously shown that individual differences are related to the presence of autistic personality traits: higher levels of autistic traits are associated with lower (superior) orientation discrimination thresholds (Dickinson et al., 2014). Here we investigate whether variability in the balance of neural excitation and inhibition (E/I) as indexed by peak gamma frequency, is associated with variability in orientation discrimination thresholds and autistic traits.

The peak frequency of gamma band (>30Hz) activity recorded using magnetoencephalography (MEG) or electroencephalography (EEG) in human subjects provides an incisive way of inferring the balance of neural excitation and inhibition (E/I). This is because oscillatory activity in the gamma frequency range is said to emerge from the interaction and balance of E/I processes (Buzsáki & Wang, 2012). Furthermore, mathematical models suggest that higher levels of inhibition are associated with a higher peak gamma frequency (Brunel & Wang, 2003). Studying peak gamma frequency can therefore provide us with a metric of the E/I balance, and an indication of whether an imbalance is caused by excessive inhibition, or excitation.

In typical observers, peak gamma frequency has been found to correlate with orientation discrimination thresholds such that higher peak gamma frequency is associated with lower thresholds (Edden et al., 2009). This relationship presumably reflects the role of neural inhibition in shaping the tuning curves of orientation selective neurons. For example, applying a GABA antagonist to block inhibition reduces orientation selectivity (e.g. Katzner et al., 2011; Sillito, 1975) whist the application of GABA leads to cells becoming more narrowly tuned (Li et al., 2008). In addition, resting levels of GABA and oblique orientation discrimination thresholds are correlated in human subjects, with higher levels of resting GABA being associated with enhanced orientation discrimination thresholds (Edden et al., 2009). Individual variability in E/I balance is therefore related to individual differences in sensory sensitivity.

Measuring peak gamma frequency allows us to investigate E/I balance on a spatial scale relevant to visual perception in human subjects, and establish whether individual variation in E/I balance may underpin the relationship between orientation discrimination thresholds and autistic traits. To our knowledge, no studies have reported peak gamma frequency either in individuals with autism spectrum conditions (ASC), or in relation to autistic traits, although in-line with existing work (Dickinson et al. 2014; Edden et al. 2009) we predict that individuals with a higher level of autistic traits will have lower orientation discrimination thresholds and a higher peak gamma frequency.

Method

Participants

Thirty-three healthy volunteers with normal or corrected to normal vision were recruited from the student and local community population (21 male, 12 female; mean age 25; age range = 18 – 45). Every participant in the current study had taken part in a previous study investigating the relationship between orientation discrimination thresholds and autistic personality traits (Dickinson et al., 2014) in which all 116 participants were given the option of taking part in an additional testing session during which EEG would be recorded. The 33 participants in the current study are those who indicated they would also like to take part in the additional EEG recording session, which was carried out on the same day. The orientation discrimination data for these participants can be found in Dickinson et al. (2014). The study received ethical approval from the Department of Psychology University of Sheffield ethics committee. Participants provided informed written consent, in accordance with the declaration of Helsinki.

Questionnaire

Participants completed the Autism Spectrum Quotient (AQ), which measures autistic traits in the general population (Baron-Cohenet al., 2001). The AQ is a self-report questionnaire in which participants state whether they agree or disagree with a series of 50 statements based around different social and communication preferences. Each statement receives a score of 0 or 1, with 1 indicating the presence of an autistic trait. The maximum score on the AQ is 50, with higher scores indicating a higher level of autistic traits.

Orientation discrimination task

Orientation discrimination thresholds were measured using a two-alternative forced choice adaptive staircase procedure based on that described by Edden and colleagues (2009) and used by Dickinson et al. (2014). The sequence of events in each trial is illustrated in figure 1. On each trial a reference grating and a target grating were presented sequentially, each for 350ms, separated by a 500ms delay. The circular gratings (diameter 4°; spatial frequency 3 cycles/degree; contrast 99%; mean luminance 83 cd/m^2) were

created in MatLab (The MathWorks Inc., Natick, MA, 2000) using the PsychToolbox set of functions (Brainard, 1997). The phase offset of each grating was randomised. Participants completed the experiment in a completely dark room. The stimuli were displayed on a linearised AMW MR19C-ABAD LCD monitor with a spatial resolution of 1280 x 1024 pixels and a temporal resolution of 60Hz. Participants were seated 57cm away from the monitor which had a circular aperture placed over it in order to remove any orientation cues provided by the edge of the screen.

Participants were asked to judge whether the target grating had been rotated clockwise or anti-clockwise compared to the reference grating. Each run consisted of four randomly interleaved staircases. There were two conditions, in one condition the reference grating was oriented at 0 degrees (vertical) and in the other it was oriented 45 degrees clockwise from vertical. Two staircases were used for each condition. One presented the clockwise transformations of the stimulus and the other presented the anti-clockwise transformations.

Responses were recorded by the participant using the left and right arrow keys on a keyboard. A one-up three-down staircase method was used, which converged on 79% correct performance (Leek, 2001). The initial target grating was presented at 5 degrees away from the reference grating. The initial step size was 1 degree which decreased by 75% after every reversal.

EEG Task

Apparatus

EEG data were collected using the BioSemi ActiveTwo system (BioSemi, Amsterdam, The Netherlands). Recordings were taken from 128 electrodes at a sampling rate of 2048Hz. All EEG was filtered online with a band pass of 0.01 -140Hz and digitised using BioSemi ActiView software. Direct current offset voltages were kept below +/- 25mV. All recordings were carried out in an electrically shielded room. Stimuli were displayed on a linearised Viglen LCD monitor with a spatial resolution of 1280 x 1024 pixels and a temporal resolution of 60Hz.

Procedure

Participants were asked to sit comfortably and keep movement to a minimum. They were instructed to fixate on a red cross in the centre of the computer monitor throughout the experiment. In order to maintain attention they were asked to respond by pressing the spacebar when a black and white grating disappeared from the screen.

Peak gamma frequency has been shown to be affected by both contrast (Ray and Maunsell, 2010) and position in space (Lima et al., 2009; van Pelt and Fries, 2013) in animal studies. We therefore used identical stimuli during the EEG recording session to Edden and colleagues (2009) who used a standardised stimulus presentation paradigm to estimate visually elicited peak gamma frequency activity in human participants using MEG. A red cross (1° x 1°) located in the centre of the screen was constantly present throughout the experiment. A black and white square grating (4° x 4°; spatial frequency 3 cycles/degree; contrast 99.6%; mean luminance 39.33 cd/m^2), located to the bottom left of the fixation cross, was repeatedly presented for between 1500 - 2500 milliseconds with an inter stimulus interval of 1500-2500ms. 200 trials were presented, separated into two blocks with a self-timed break in between. Participants were instructed to respond to first half of the trials using their right hand, and the second half using their left hand. Participants sat 57cm away from the monitor, at this distance the stimuli subtended by 4 visual degrees.

Problems of measuring induced gamma activity

EEG recorded at the scalp is a linear mixture of several sources of neural activity, as well as several sources of non-neural artifcat. Electrooculography (EOG) and electromyography (EMG) artifacts are highly prevalent in the EEG signal. In addition, there are also artifacts which are particularly problematic for the current investigation as they share a similar frequency range to the gamma band of interest. For instance power line interference causes artifacts throughout the EEG signal at 50Hz. In addition, there have been previous reports of EEG power changes in the gamma frequency range between 200 and 300ms post stimulus onset that are related to saccadic eye movements (Yuval-Greenberg, Tomer, Keren, Nelken & Deouell, 2008). Power line interference and the saccadic spike potential (SP) would therefore overlap with both the time and frequency range of interest here (>30Hz).

A solution to this problem is to use independent component analysis (ICA), a statistical blind source separation technique, to decompose the EEG recording into maximally independent components (Makeig, Jung, Bell, Ghahremani & Sejnowski, 1997) Analysing data from a single independent component for each participant which best represented the visual response to the stimuli allowed us to isolate the visual response and eliminate artifacts including EMG, EOG, the SP and the small amount of residual 50Hz power line interference that resisted shielding.

EEG Analysis

Continuous EEG data were down-sampled from 2048Hz to 1024Hz using BioSemi DBF Decimator software. The rest of the offline data analysis was performed using EEGLAB (Delorme & Makeig, 2004), and in-house MATLAB scripts. Data were referenced to the vertex electrode and high pass filtered to remove frequencies below 1Hz, using a finite impulse response filter, as implemented in EEGLAB. Data were then visually screened and any artifactual channels or segments of data were removed. After removing artifactual channels an average of 117 channels (SD = 8.27, range = 91 - 127) remained for each participant.

Data were then segmented into epochs (-200 -1500 ms) corresponding to the presentation of the stimulus at 0ms. Any trials in which the participant did not respond within 1500ms following stimulus-offset were removed. After this process an average of 185 epochs per participant remained (SD = 11.58, range = 149 – 200).

After epoching, extended infomax ICA was carried out using EEGLAB (Delorme & Makeig, 2004). Finally, the source location for each independent component was estimated using the DIPFIT function in EEGLAB. DIPFIT estimates the anatomical location using inverse source modelling by creating an equivalent current dipole model which best represents the scalp topography of each independent component, applied to a standard boundary head model (Oostendorp & Van Oosterom, 1989).

We then used a standardised process (described below) to select a single component for each participant for gamma-band analysis.

Independent Component Selection

The scalp topography of each component was visually inspected. Any components which had focal activity in the occipital cortex which was lateralised to the right hemisphere were initially selected. This led to up to 8 components being selected for each participant (M = 4.33, SD = 1.53, range = 2 - 8). The time course of each of the selected components was used to exclude any components without a clear visual evoked potential. This led to up to 4 components being retained for each participant (M = 2.03, SD = .81 , range= 1 - 4). Time frequency analysis (described below) was then performed on each of the remaining components. Any components which did not show a stimulus elicited change in oscillatory gamma activity were excluded. The final component for each participant was selected on the grounds of the clearest sustained visually elicited change in gamma power. The final component was chosen out of a maximum of 3 components per participant (M = 1.64, SD = .70, range=1 - 3).

To summarise, for each participant a single independent component was selected on the basis of it reflecting a source of activity in or near right occipital cortex and demonstrating visually-induced neural activity, including an increase in post-stimulus gamma-band power. Component selection was carried out while the experimenter was blind to both the AQ score and orientation-discrimination threshold of the participant.

Time-Frequency Analysis

The time series of the selected independent component from each subject was then analysed in the time-frequency domain using wavelet transforms. Wavelet methods offers advantages over windowed fourier methods in that each wavelet is specific to both time and frequency and is not subject to edge effects. It has advantages over multitaper methods in that less effective smoothing in both time and frequency occurs thus offering greater spectral and temporal resolution (Cohen, 2014). The complex Morlet wavelet (a complex exponential modulated by a Gaussian, $\omega 0 = 6$; where $\omega 0$ is nondimensional frequency) was chosen as the function $\psi 0$ because it provides a good balance between time and frequency localisation for feature extraction purposes (Grinsted, Moore & Jevrejeva, 2004; Müller et al., 2004). The complex Morlet wavelet is described by the following function:

$$\psi_0(\eta) = \pi^{-1/4} e^{i\omega_0 \eta} e^{-\eta^2/2} \quad \textbf{1}$$

The wavelet transform $W^x(n,s)$ is a complex quantity whose modulus expresses the amount of power in x and whose angle represents the local phase localised in time and frequency (scale). Scale determines the temporal resolution of the analysis. The continuous wavelet transform of a time series x_n of N subsampled data points at equal time increments of δt (Kaiser, 1994), is defined as the convolution of x_n with a scaled and translated version of ψ_0:

$$W^x(n,s) = \sqrt{\frac{\delta t}{s}} \sum_{n'-1}^{N} x_{n'} \psi_0^* \left[\frac{(n'-n)\delta \mathrm{t}}{s} \right] \quad \textbf{2}$$

where ψ_0^* is the complex conjugate of ψ_0, n is the time index and s denotes the wavelet scale. The set of scales were chosen such that the number of octaves per scale was set at 1/60 which provided a sufficiently 'smooth' picture of wavelet power and resulted in sufficient spectral resolution in the Gamma range for the purposes of the present investigation (<1Hz). The time series of the selected component for each subject for each stimulus presentation trial was analysed using this wavelet method. The mean values of power for each scale during the pre-stimulus period for each trial was considered to be baseline and was subtracted from the wavelet transforms. As such, data is presented as changes in power following stimulus presentation (see Figure 2). For each subject the wavelet transforms were performed on each epoch and were then trial-averaged to increase signal to noise ratio. A curve was fitted to the spectra at the time point associated with the maximum increase in gamma power following stimulus presentation using non-linear least squares. The single frequency associated with the maximum of this fitted curve was taken as the metric of peak gamma frequency for each subject (see figure 2C).

Results

AQ scores ranged from 6 to 42 (M= 19.3, SD = 10.5). The mean orientation discrimination threshold in the vertical and oblique conditions condition was 1.53 ± 1.09° (range = .44 – 5.41 °) and 5.69 ± 2.52° (range = 2.32 – 11.56°) respectively. A classic oblique effect was observed as orientation discrimination thresholds were significantly higher in the oblique condition than in the vertical condition, t (32) = -11.391, p = <.0001. Given that the oblique condition provides a more sensitive indication of orientation discrimination than the vertical condition (Dickinson et al., 2014) only oblique thresholds were used in further analyses. We checked for any potential attention related effects on performance by comparing individuals' thresholds on the first and second runs of the orientation discrimination task. There was no difference between mean scores on the first (M=5.94, SD=2.77) and second run (M=5.45, SD=2.55) (t(32)=1.66, p=.1). AQ score was not correlated with the difference between the two runs (r=.298, p=.09).

Peak gamma frequency ranged from 30.27 to 89.66Hz (M=59.37, SD=15.66). As peak gamma frequency has been shown to be related to attention in animal studies, (Bosman et al., 2012), we checked whether peak gamma frequency when calculated from the first and second halves of the EEG recording was consistent. Specifically, we were keen to ensure that individual differences in levels of attention could not account for the relationship between peak gamma frequency and AQ score. Wavelet analyses as described in the method section were carried out separately for the first and second half of trials. The second half of trials had a slightly higher peak gamma frequency (M=61.51, SD=15.39) than the first half (M=57.61, SD=18.36), but this difference was not statistically significant (t(32)=-1.492, p=.146). Importantly, the difference between the peak gamma frequency for the first and second half of trials was also unrelated to AQ score (r=-.04, p=.822).

There was a significant negative correlation between oblique orientation discrimination thresholds and AQ score (r=-.492, p=.004, Figure 3A). Note that the data reported here represent a subset of a larger dataset reported elsewhere (Dickinson et al., 2014), therefore we highlight that a significant correlation between these two variables was still observed even in this restricted number of participants. As hypothesised, there was also a significant negative correlation between peak induced gamma frequency and

oblique orientation discrimination threshold (r=-.526, p=.002, Figure 3B), and a significant correlation between AQ score and peak induced gamma frequency (r=.582, p=<.001, figure 3C).

Discussion

Here we show that individual differences in peak gamma frequency are related to both autistic traits and oblique orientation discrimination thresholds. Orientation discrimination thresholds have previously been found to be lower in those with higher levels of autistic traits (Dickinson et al., 2014) and lower in those with higher peak gamma frequencies (Edden et al., 2009). Therefore, we predicted that peak gamma frequency would be higher in those with higher levels of autistic traits; this prediction was supported by the data. These data also replicate existing work by showing a significant negative correlation between orientation discrimination thresholds and peak gamma-frequency (Edden et al., 2009).

Modelling work demonstrates that the frequency of gamma-band oscillations is affected by the balance between excitatory and inhibitory processes. Both a higher ratio of inhibition to excitation, and faster inhibition than excitation have been said to lead to a higher peak gamma frequency (Brunel & Wang, 2003). Given the role of inhibition in shaping orientation selectivity, the relationship between orientation discrimination thresholds and peak gamma frequency also supports that higher levels of inhibition are associated with a higher peak gamma frequency (Edden et al., 2009). Therefore we suggest that a higher level of autistic traits may indicate an increase in neural inhibition. Increased inhibition may be mediated through a number of means, including increased levels of GABA, reduced levels of glutamate, or atypical lateral connectivity.

One body of work suggests that it is variation in GABA levels specifically that may drive individual differences in peak gamma frequency (Chen et al., 2014; Muthukumaraswamy, et al., 2009; Edden et al., 2009). However, this claim has recently been put into question by a study which failed to find any relationship between peak gamma frequency and resting GABA levels measured using magnetic resonance spectroscopy (MRS; Cousijn et al., 2014). It is important to note that there are limitations to measuring GABA in human participants, as MRS measures a mix of macromolecules and homocarnosine, as well as GABA (Gao et al., 2013). Also, MRS measures GABA in a relatively large area of brain ($27cm^3$), and it can be hard to localise such a large voxel to a particular cortical area (Puts & Edden, 2012). Therefore, in-light of the work from Cousijn and colleagues (Cousijn et al., 2014), we remain open to the possibility that other

causal factors may drive individual differences in inhibition, including structural differences which may also impact excitatory and inhibitory processes. For instance, V1 size has also been shown to correlate with peak gamma frequency (Schwarzkopf et al., 2012). Peak gamma frequency has also been found to have a strong genetic determination, with a heritability of around 91% (van Pelt et al., 2012).

Our study is the first to investigate peak gamma frequency in relation to autistic traits, and we suggest it is a technique which could help shed light on the postulated disruption to E/I balance in ASC. Due to interest in the E/I balance, gamma-band activity has been extensively studied in individuals with ASC (e.g. Orekhova et al., 2007; Grice et al., 2001), and is said to be atypical (Uhlhaas & Singer, 2006). However, all previous studies of gamma oscillations in ASC have reported gamma power and not gamma frequency. Here, we demonstrate that peak gamma-frequency may be a useful metric for the study of E/I in ASC.

When considering the implications of this finding to the understanding of ASC, it is reasonable to predict that individuals with ASC will show enhanced perceptual discrimination, and to suggest that this is underpinned by increased neural inhibition. It is certainly the case that lower perceptual thresholds have been reported in those with ASC across a number of domains including orientation discrimination (Bertone et al., 2005) pitch discrimination (Heaton, Hermelin & Pring, 1998; see Haesen, Boets & Wagemans, 2011, for a review) and somatosensory discrimination (Cascio et al., 2008). On the basis of these data, it has previously been suggested that inhibition might be increased in ASC.

Bertone and colleagues (2005) postulated that higher levels of lateral inhibition exist in individuals with ASC due to atypical neural connectivity. In support of this claim, studies employing psychophysical paradigms such as crowding and lateral masking suggest that lateral connectivity, which is mediated by E/I interactions, is altered in those with ASC (Kéïta et al., 2011). However, this suggestion is at odds with a prominent theory suggesting that inhibition is reduced in ASC, leading to cortical hyperexcitability (Rubenstein & Merzenich, 2003). Clearly, the theory of reduced neural inhibition is incompatible with evidence of superior perceptual discrimination in ASC (c.f. Dickinson & Milne, 2014). A small number of studies have attempted to measure inhibition in ASC directly by using MRS to measure levels of resting

state GABA (Gaetz et al., 2014; Harada et al., 2011; Rojas et al., 2014). Results are generally in favour of lower levels of GABA in ASC at least in the motor cortex (Gaetz et al., 2014) and auditory cortex (Gaetz et al., 2014: Rojas et al., 2014), but not in the occipital cortex (Gaetz et al., 2014). However, as noted above there are limitations of measuring GABA in human subjects therefore it may be worth exercising caution when drawing conclusions about neural inhibition from measures of GABA until the techniques have been refined.

Further work is clearly needed to establish whether inhibitory or excitatory processes are altered in ASC, and if so, through which mechanisms. Here we raise the issue that although the theory of reduced inhibition / increased excitation has been highly influential in the field of autism research, evidence from sensory discrimination thresholds in ASC is not in-line with this claim. Our current finding that high levels of autistic traits are associated with both lower orientation discrimination thresholds and higher peak gamma frequencies is not consistent with this theory as it suggests increased, rather than decreased, levels of inhibition. Given that some individuals with ASC also have lower discrimination thresholds (Bertone et al., 2005; Cascio et al., 2008; Heaton, Hermelin & Pring, 1998), we highlight that it is important to revisit the assumption that ASC is associated with reduced levels of inhibition.

To conclude, here we find that individual differences in autistic traits are associated with variability in both orientation discrimination thresholds and peak gamma frequency. This leads to the novel hypothesis that inhibition levels may also mediate levels of autistic traits. Ours and others work suggests that measuring peak gamma frequency represents a promising technique for investigating a putative E/I imbalance in ASC. Specifically, we suggest that higher levels of inhibition are associated with the presence of autistic traits.

References

Baron-Cohen, S., Wheelwright, S., Skinner, R., Martin, J. & Clubley, E. (2001). The autism-spectrum quotient (AQ): Evidence from asperger syndrome/high-functioning autism, malesand females, scientists and mathematicians. *J Autism Dev Disord.*, **31(1)**, 5-17.

Bertone, A., Mottron, L., Jelenic, P., & Faubert, J. (2005). Enhanced and diminished visuo-spatial information processing in autism depends on stimulus complexity. *Brain*, **128(10)**, 2430-2441.

Bosman, C. A., Schoffelen, J. M., Brunet, N., Oostenveld, R., Bastos, A. M., Womelsdorf, T., ... & Fries, P. (2012). Attentional stimulus selection through selective synchronization between monkey visual areas. *Neuron*, **75(5)**, 875-888.

Brainard, D. H. (1997). The psychophysics toolbox. *Spatial vision*, **10**, 433-436.

Brunel, N. & Wang, X. J. (2003). What determines the frequency of fast network oscillations with irregular neural discharges? I. Synaptic dynamics and excitation-inhibition balance. *J neurophysiol*., **90(1)**, 415-430.

Buzsáki, G. & Wang, X. J. (2012). Mechanisms of gamma oscillations. *Annu rev neurosci*., **35**, 203-225.

Cascio, C., McGlone, F., Folger, S., Tannan, V., Baranek, G., Pelphrey, K. A. & Essick, G. (2008). Tactile perception in adults with autism: a multidimensional psychophysical study. *J Autism Dev Disord.*, **38(1)**, 127-137.

Chen, C. M. A., Stanford, A. D., Mao, X., Abi-Dargham, A., Shungu, D. C., Lisanby, S. H. ... & Kegeles, L. S. (2014). GABA level, gamma oscillation, and working memory performance in schizophrenia. *NeuroImage: Clinical*, **4**, 531-539.

Cohen, M. X. (2014). *Analyzing neural time series data: theory and practice*. MIT Press.

Cousijn, H., Haegens, S., Wallis, G., Near, J., Stokes, M. G., Harrison, P. J. & Nobre, A. C. (2014). Resting GABA and glutamate concentrations do not predict visual gamma frequency or amplitude. *PNAS.*, **111(25)**, 9301-9306.

Delorme, A. & Makeig, S. (2004). EEGLAB: an open source toolbox for analysis of single-trial EEG dynamics including independent component analysis. *J. Neurosci. Method.s*, **134(1)**, 9-21.

Dickinson, A. & Milne, E. (2014). Enhanced and impaired sensory discrimination in autism. *J. neurophysiol*., **112(6)**, 1599-1599.

Dickinson, A., Jones, M. & Milne, E. (2014). Oblique Orientation Discrimination Thresholds Are Superior in Those with a High Level of Autistic Traits. *J Autism Dev Disord.*, **44 (11)**, 2844 - 2850.

Edden, R. A., Muthukumaraswamy, S. D., Freeman, T. C. & Singh, K. D. (2009). Orientation discrimination performance is predicted by GABA concentration and gamma oscillation frequency in human primary visual cortex. .*J. Neurosci.*, **29(50)**, 15721-15726.

Gaetz, W., Bloy, L., Wang, D. J., Port, R. G., Blaskey, L., Levy, S. E. & Roberts, T. P. L. (2014). GABA estimation in the brains of children on the autism spectrum: measurement precision and regional cortical variation. *Neuroimage,* **86**, 1-9.

Gao, F., Edden, R. A., Li, M., Puts, N. A., Wang, G., Liu, C. ... & Barker, P. B. (2013). Edited magnetic resonance spectroscopy detects an age-related decline in brain GABA levels. *Neuroimage*, **78**, 75-82.

Grice, S. J., Spratling, M. W., Karmiloff-Smith, A., Halit, H., Csibra, G., de Haan, M. & Johnson, M. H. (2001). Disordered visual processing and oscillatory brain activity in autism and Williams syndrome. *Neuroreport*, **12(12)**, 2697-2700.

Grinsted, A., Moore, J. C. & Jevrejeva, S. (2004). Application of the cross wavelet transform and wavelet coherence to geophysical time series. *Nonlinear Process Geophys.*, **11(5/6)**, 561-566.

Haesen, B., Boets, B. & Wagemans, J. (2011). A review of behavioural and electrophysiological studies on auditory processing and speech perception in autism spectrum disorders. *Research in Autism Spectrum Disorders.*, **5(2)**, 701-714.

Halpern, S., Andrews, T. & Purves, D. (1999). Interindividual variation in human visual performance. *J. Cogn. Neurosci.*, **11(5)**, 521-534.

Harada, M., Taki, M. M., Nose, A., Kubo, H., Mori, K., Nishitani, H. & Matsuda, T. (2011). Non-invasive evaluation of the GABAergic/glutamatergic system in autistic patients observed by MEGA-editing proton MR spectroscopy using a clinical 3 tesla instrument. *J Autism Dev Disord.*, **41(4)**, 447-454.

Heaton, P., Hermelin, B. & Pring, L. (1998). Autism and pitch processing: A precursor for savant musical ability? *Music percept.*, **15**, 291-305.

Hubel, D. H. & Wiesel, T. N. (1968). Receptive fields and functional architecture of monkey striate cortex. *J. Physiol.*, **195(1)**, 215-243.

Kaiser, G. (2010). *A friendly guide to wavelets*. Springer.

Katzner, S., Busse, L. & Carandini, M. (2011). GABAA inhibition controls response gain in visual cortex. .*J. Neurosci.*, **31(16)**, 5931-5941.

Kéïta, L., Mottron, L., Dawson, M. & Bertone, A. (2011). Atypical lateral connectivity: a neural basis for altered visuospatial processing in autism. *Biol. Psychiatry*., **70(9)**, 806-811.

Leek, M. R. (2001). Adaptive procedures in psychophysical research. *Percept. Psychophys.*, **63(8)**, 1279-1292.

Li, G., Yang, Y., Liang, Z., Xia, J., Yang, Y. & Zhou, Y. (2008). GABA-mediated inhibition correlates with orientation selectivity in primary visual cortex of cat. *Neuroscience*, **155(3)**, 914-922.

Lima, B., Singer, W., Chen, N. H., & Neuenschwander, S. (2010). Synchronization dynamics in response to plaid stimuli in monkey V1. *Cerebral cortex*, **20(7)**, 1556-1573.

Makeig, S., Jung, T. P., Bell, A. J., Ghahremani, D. & Sejnowski, T. J. (1997). Blind separation of auditory event-related brain responses into independent components. *PNAS,* **94(20)**, 10979-10984.

MATLAB, 6.1, The MathWorks Inc., Natick, MA, 2000.

Müller, K., Lohmann, G., Neumann, J., Grigutsch, M., Mildner, T. & Von Cramon, D. Y. (2004). Investigating the wavelet coherence phase of the BOLD signal. *J. Magn. Reson.*, **20(1)**, 145-152.

Muthukumaraswamy, S. D., Edden, R. A., Jones, D. K., Swettenham, J. B. & Singh, K. D. (2009). Resting GABA concentration predicts peak gamma frequency and fMRI amplitude in response to visual stimulation in humans. *PNAS*, **106(20)**, 8356-8361.

Oostendorp, T. F. & Van Oosterom, A. (1989). Source parameter estimation in inhomogeneous volume conductors of arbitrary shape. *IEEE Trans. Biomed. Eng.*, **36(3)**, 382-391.

Orekhova, E. V., Stroganova, T. A., Nygren, G., Tsetlin, M. M., Posikera, I. N., Gillberg, C. & Elam, M. (2007). Excess of high frequency electroencephalogram oscillations in boys with autism. *Biol. psychiatry*, **62(9)**, 1022-1029.

Puts, N. A. & Edden, R. A. (2012). < i> In vivo</i> magnetic resonance spectroscopy of GABA: A methodological review. *Prog. Nucl. Magn. Reson. Spectrosc.*, **60**, 29-41.

Ray, S., & Maunsell, J. H. (2010). Differences in gamma frequencies across visual cortex restrict their possible use in computation. *Neuron*, **67(5)**, 885-896.

Rojas, D. C., Singel, D., Steinmetz, S., Hepburn, S. & Brown, M. S. (2014). Decreased left perisylvian GABA concentration in children with autism and unaffected siblings. *Neuroimage*, **86**, 28-34.

Rubenstein, J. L. R. & Merzenich, M. M. (2003). Model of autism: increased ratio of excitation/inhibition in key neural systems. *Genes Brain Behav.*, **2(5)**, 255-267.

Schwarzkopf, D. S., Robertson, D. J., Song, C., Barnes, G. R. & Rees, G. (2012). The frequency of visually induced gamma-band oscillations depends on the size of early human visual cortex. *J. Neurosci.*, **32(4)**, 1507-1512.

Sillito, A. M. (1975). The contribution of inhibitory mechanisms to the receptive field properties of neurones in the striate cortex of the cat. *J. Physiol.*, **250(2)**, 305-329.

Uhlhaas, P. J. & Singer, W. (2006). Neural synchrony in brain disorders: relevance for cognitive dysfunctions and pathophysiology. *Neuron*, **52(1)**, 155-168.

van Pelt, S., & Fries, P. (2013). Visual stimulus eccentricity affects human gamma peak frequency. *Neuroimage,* **78,** 439-447.

van Pelt, S., Boomsma, D. I., & Fries, P. (2012). Magnetoencephalography in twins reveals a strong genetic determination of the peak frequency of visually induced gamma-band synchronization. The Journal of *Neuroscience,* **32(10)**, 3388-3392.

Yuval-Greenberg, S., Tomer, O., Keren, A. S., Nelken, I. & Deouell, L. Y. (2008). Transient induced gamma-band response in EEG as a manifestation of miniature saccades. *Neuron*, **58(3)**, 429-441.

Figures

Figure 1. Schematic diagram of the orientation discrimination task.

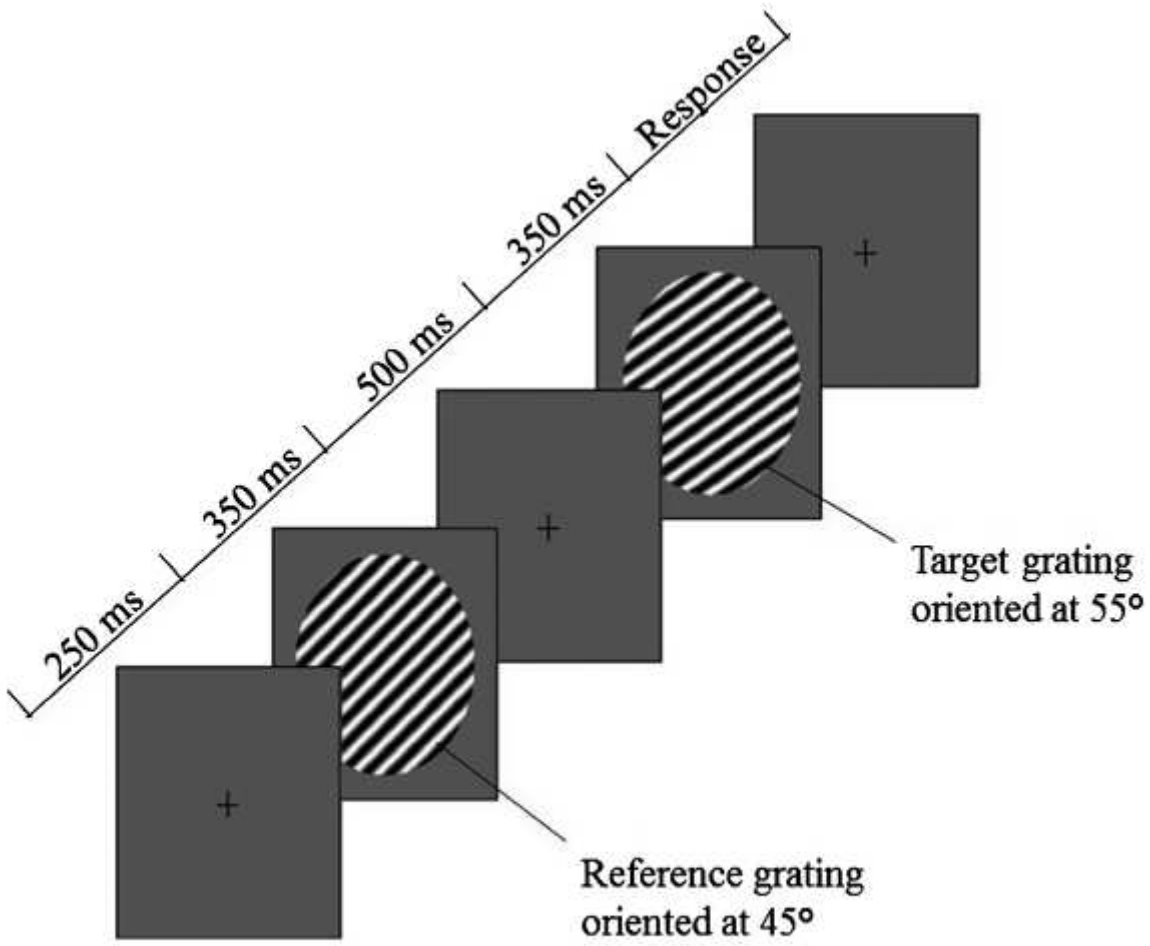

FIG. 1. Schematic diagram of the orientation discrimination task.

Figure 2. (A) Time frequency decomposition and scalp map of the selected component of a subject with a low AQ score. (B) Time frequency decomposition and scalp map of the selected component of a subject with a high AQ score. (C) The total power change at each frequency for the low (plotted in blue) and high (plotted in red) subjects plotted in 2A and 2B.

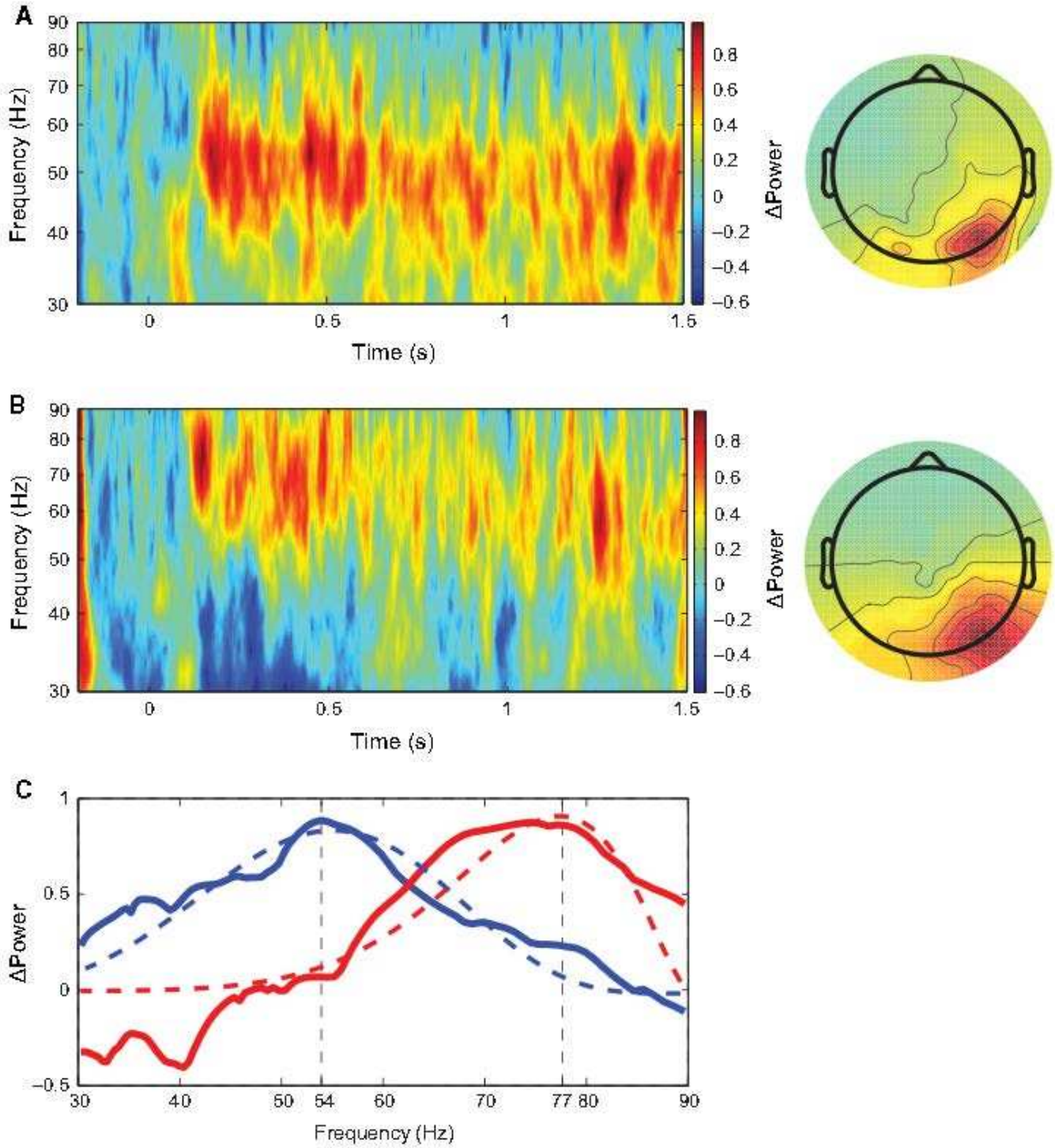

Figure 3. (A) Correlation between oblique orientation discrimination threshold and AQ score (N=33). (B) Correlation between oblique orientation discrimination threshold and peak gamma frequency (N=33). (C) Correlation between peak gamma frequency and AQ score (N=33).

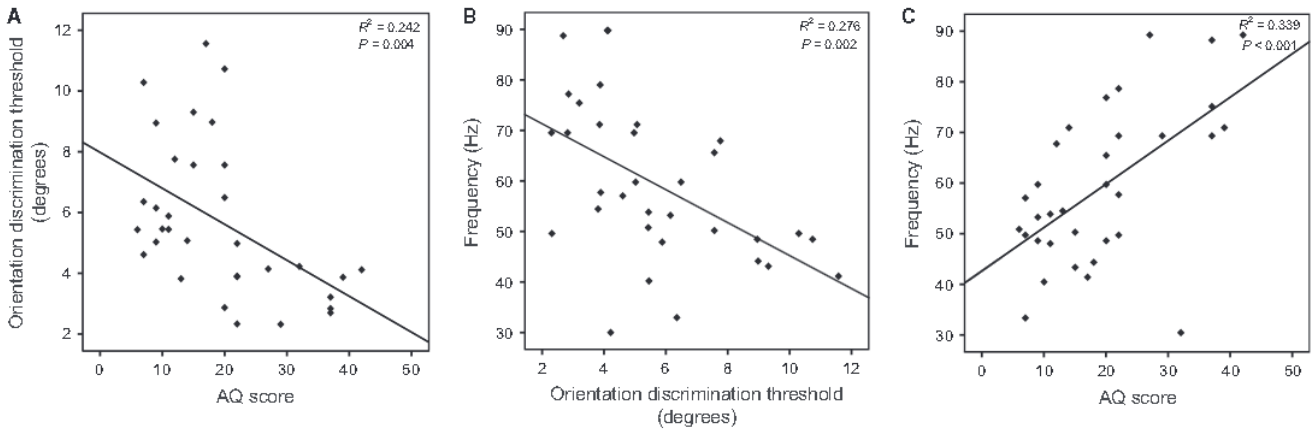
A
R^2 = 0.242
P = 0.004
Orientation discrimination threshold (degrees)
AQ score
B
R^2 = 0.276
P = 0.002
Frequency (Hz)
Orientation discrimination threshold (degrees)
C
R^2 = 0.339
P < 0.001
Frequency (Hz)
AQ score